Case Studies in Thermal Engineering 41 (2023) 102691

Contents lists available at ScienceDirect

Case Studies in Thermal Engineering

journal homepage: www.elsevier.com/locate/csite

Analytical model for extremum analysis of moistened fins involving all nonlinear energy exchange processes

Balaram Kundu [a], Se-Jin Yook [b,*]

[a] Department of Mechanical Engineering, Jadavpur University, Raja S. C. Mallick Road, Kolkata, West Bengal, 700032, India
[b] School of Mechanical Engineering, Hanyang University, 222 Wangsimni-ro, Seongdong-gu, Seoul, 04763, Republic of Korea

GRAPHICAL ABSTRACT

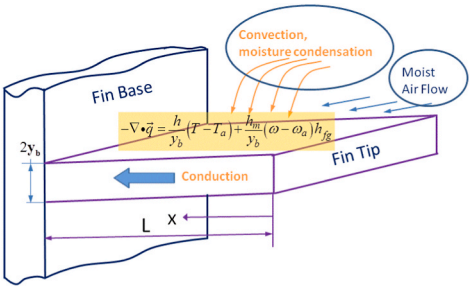

ARTICLE INFO

Handling Editor: Huihe Qiu

Keywords:
Analytic
Decomposition method
Nonlinear convection coefficients
Variable thermal conductivity
Heat load
Moistened fin

ABSTRACT

Dehumidification on a fin surface happens when the thermal interface state maintains an undervalue corresponding to saturation condition, and a temperature boundary layer develops during heat transmission. The local thickness of the temperature boundary layer changes, and consequently, sensible and latent heat transfer coefficients become highly non-uniform. In this study, a new mathematical procedure depending on the Adomian decomposition method (ADM) is established to predict the heat transfer duty from a moistened fin where all heat transfer modes involved are functions of temperature. A cubic algebraic equation for connecting the specific humidity of air and the thermal state level of a fin is closer to the actual relation determined based on the regression analysis, which converts the governing equation into a highly nonlinear character. The present model has no restriction using the fractional power factor of temperature-dependent convection coefficients. The current results highlight that the variable convection coefficients decrease both the fin performance index and heat load rate, and this influence becomes significant at the optimum design condition. Therefore, establishing the optimum state of a fin adopting all the variability events in the practical design system is essential for the correct

* Corresponding author.
E-mail address: ysjnuri@hanyang.ac.kr (S.-J. Yook).

https://doi.org/10.1016/j.csite.2022.102691
Received 6 October 2021; Received in revised form 27 December 2022; Accepted 29 December 2022
Available online 30 December 2022

analysis. As the equipment implementation analysis always requires an extremum study, the proposed research will help to predict the optimum information in the practical design with the highest accurate prediction of results.

Nomenclature

A, B, C, D	variables involved for expressing the moisten of saturation curve, defined in Eq. (2)
Bi	Biot Number
c_p	heat capacity per unit mass at a fixed pressure ($Jkg^{-1}K^{-1}$)
f	constraint function defined in Eq. (32)
g	optimality condition written in Eq. (30)
h	coefficient of convection ($Wm^{-2}K^{-1}$)
h_b	coefficient of convection at the base surface ($Wm^{-2}K^{-1}$)
h_{fg}	specific enthalpy during the vaporization of water ($J\ kg^{-1}$)
h_m	coefficient of mass transfer for the condensation ($kg\ m^{-2}s^{-1}$)
J	Jacobian determinant
k	coefficient of localised conduction ($Wm^{-1}\ K^{-1}$)
k_b	thermal conductivity at the base temperature ($Wm^{-1}\ K^{-1}$)
K_0, K_1, K_2, K_3	constants as defined in Eq. (11), $K_i = \delta_i/(1+\beta), i = \{0,1,2,3\}$
L	fin length (m)
Le	Lewis number, ratio of molecular diffusivity of heat to molecular diffusivity of mass
m	index of variability nature of convection
p_a	total pressure (kPa)
q	actual heat load (W)
q_i	ideal heat load (W)
Q	normalized actual heat load through a fin divided by width, $q/[2k_b(T_a - T_b)]$
Q_i	normalized ideal heat load divided by width, $q_i/[2k_b(T_a - T_b)]$
RH	relative humidity
T	thermal state temperature of a fin dependent on coordinate (^0C)
T_a	surrounding fluid temperature (^0C)
T_b	fin temperature at the base (^0C)
T_d	saturation temperature of air (^0C)
T_t	temperature of a fin at the tip (^0C)
U	normalized volumetric size of a fin divided by width, h^2V/k_b^2
V	Volumetric size of a fin divided by width (m^2)
x	Cartesian coordinate (m)
X	normalized Cartesian coordinate, x/L
y_b	half-thickness dimension of a fin (m)
Z_0	normalized input fin parameter, $\sqrt{Bi}/\psi$

Greek Letters

α	variable thermal conductivity parameter ($^0C^{-1}$)
β	normalized parameter to describe variational effects of coefficient of heat conductivity, $\alpha(T_a - T_b)$
$\delta_0, \delta_1, \delta_2, \delta_3$	constants described in Eq. (5)
ε	effectiveness parameter by considering a fin
η	fin efficiency
θ	normalized fin thermal state, $(T_a - T)/(T_a - T_b)$
θ_t	normalized tip thermal state of a fin, $(T_a - T_t)/(T_a - T_b)$
ξ	latent heat load factor, $h_{fg}/(c_pLe^{2/3})(^0C)$
φ	relative moisture content of surrounding air
ψ	normalized base thickness or aspect ratio, y_b/L
ω	absolute psychrometric moisture content of saturated air

ω_a	absolute psychrometric moisture content of ambient air
Δ	Second-order operator

Subscripts

a	surrounding
b	base
d	saturation
t	tip

1. Introduction

The attachment of a fin is a passive technique for augmenting heat transfer duty from a surface under a necessity design. In refrigerating, air conditioning, and aerospace systems, the cooling coil with fins reduces the surrounding fluid temperature below the ambient value to maintain a desired thermal condition. The surrounding humid air temperature reduces when it contacts the fin surface in the above applications. During this event, the boundary layer forms for fluid and heat movement for the viscosity, and a temperature gradient exists in the fluid. Suppose a fin's local thermal state temperature is kept lower than the dewpoint value. In that case, the condition is favourable to condense water vapour; thus, diffusion events exhibit. For the development of different layers, the uniformity of coefficients for convection processes deviates owing to the different thermal resistances developed for the heat flow. The coefficient of thermal diffusion also changes with the temperature variability in the fin, which becomes predominant depending on the fin material utilized in design cases.

The wet fin with heat load duty involves a complex phenomenon for the governing energy transfer equation associated with the two unknown dependent variables: temperature and moisture. Therefore, estimating the exact thermal field in the fin always requires the moisture content parameter of adjacent humid air to be expressed as a nonlinear algebraic function of temperature. For the moisture to condense, the solid fin surface is surrounded by saturated air. Hence, psychometric connectivity between specific humidity and saturation temperature can be used to determine unknown fin temperatures. The previous studies establish that the linear dependency of specific humidity on the local fin temperature is not the appropriate selection. Instead, it is always nonlinearly dependent and obtains exactly from the psychometric relation. Hence, a polynomial relationship gives a much better approximation [1]. The analytical solution of wet fins with different geometries under the mass transfer event includes the non-linear terms in the governing differential equations [2]. Earlier research works already reported the influence of moisture condensed on the performance indicator of fins. Threlkeld [3], McQuiston [4], Kilic and Onat [5], Elmahdy and Briggs [6], Coney et al. [7,8], Srinivasan and Shah [9], etc. investigated the performance parameters of wet fins. Wu and Bong [10] introduced a partially moist fin and indicated that the efficiency of a moist fin is greatly affected by the surrounding humid air. Further research works on annular fins, and fin assemblies of different profiles under dehumidification were carried out by Kazeminejad [11], Kazeminejad et al. [12], Hong and Webb [13], Salah El-Din [14], Rosario and Rahman [15], etc.

Kundu [16] studied the design analysis of a variable thickness longitudinal moistening fin for the first time. He showed that the moistened fin performance indicator is lesser than the dry surface fin. He also revealed that the geometric dimensional ratio of an extended surface under the dehumidification of moist air is always higher to increment the heat transfer rate than the dry fin for the identical volume and thermo-physical parameters. The Maple software-based Finite Difference Method used to solve the nonlinear partial differential equation for a porous longitudinal fin in a thoroughly wet condition was modeled by Sowmya et al. [17] in the existence of convection and radiation modes of heat transfer. Naphon [18] presented an analysis theoretically to characterize the heat transport and performance indicator of annular fin arrays under different conditions of heat transfer surfaces. Using a simple correlation, Nemati and Samivand [19] evaluated the efficiency of annular oval fins on a circular tube considered a base surface.

Turkyilmazoglu [20] determined the optimum fin dimensions of a parabolic pin fin under a uniform oncoming airflow by maximizing the base heat transfer rate with the variation of the Peclet number. Kundu [21] analyzed the heat transfer mechanism for the optimum noneccentric circular wet fins. He proposed an alternative geometry of circumferential fins by adopting the design aspects, the ease of manufacturing, and material utilization in conducting heat near the tip. Most researchers assumed the tip temperature and saturation temperature equality, which is only sometimes satisfied. He demonstrated an iterative scheme for the actual thermal state of fins. To eliminate tedious iterative steps, Sharqawy and Zubair [22,23] assumed that a fully moist fin equals tip and saturation temperature. As the tip state temperature always differs from the saturation value, the assumption by Sharqawy and Zubair is approximate. The above literature works for the moistened fin were illustrated with a linear mathematical function between the mass transfer potential and sensible heat transfer potential. Recently, Sowmya et al. [24] numerically examined a porous circumferential fin under fully moist conditions with SWCNTs, MWCNTs, and internal heat generation.

The absolute humidity as a temperature-dependability function can be obtained from the psychometric chart. The best fit method provided a relationship which is a polynomial function. Kundu [1] applied an analytical method for analysing straight moisten-fins with the above relation. He also conducted a thermal study for design performance indexes for mixed dry and wet conditions of a fin by establishing a new scheme. Using the Homotopy analysis method, Moradi et al. [25] determined the heat duty through a fin with moving states whereas Roy et al. [26] demonstrated a modified analytical solution for tapered moving fins. Chiu and Chen [27]

investigated the temperature pattern in a rectangular dry fin using ADM, and they optimized the geometric shape of a fin. The thermal energy transfer efficiency of a dry fin with the variable conduction property was evaluated by Arslanturk [28]. He found that the variability nature of the thermal conductivity has a powerful dependability function with the heat transfer process. Using the same mathematical technique, Chang [29] modeled for evaluating the thermal behaviour of a dry fin for variable heat transfer coefficients. In recent work, Kundu and Yook [30] recommended a modification of the analysis for all types of porous fins by eliminating all physical and mathematical errors existed in the available literature. A suitable analytical method was proposed for the design criterion of three common types of porous fins having all nonlinearity events and formulated in a generalized way. The justification for the modification required was highlighted and presented.

By applying the least square method, Vahabzadeh et al. [31] determined the temperature distribution, heat transfer rate, efficiency, and optimization of porous pin fins in fully wet conditions. A combination of the differential transform method (DTM) and finite difference method (FDM) was utilized as a solution technique by Peng and Chen [32] to investigate a circumferential dry fin that dissipates heat by convection and radiation. Domairry and Fazeli [33] studied a straight dry fin with changeable thermal conductivities by homotopy analysis. Based on a DTM analysis, Babaelahi and Raveshi [34] determined the efficiency of an aerospace radiating fin. Using a numerical relaxation scheme, Rusagara and Harley [35] solved the transient heat transfer equation for exponential fins.

Cuce and Cuce [36] used a novel approach by the Homotopy perturbation technique for analysing dry fin with the nonlinear heat conduction effect. But, Ma et al. [37] examined the multidimensional heat flow and non-uniform heat transfer coefficients for an unvarying thickness dry fin. They studied the effect of three general boundary conditions at the tip. Dul'kin and Garas'ko [38,39] assumed the coefficient of the convective heat transfer that varies according to the temperature-dependent power factor in a given range. They investigated different dry fins of unvarying thickness. They also studied the optimization of straight-plate and cylindrical-pin fin geometries with the adiabatic and diabetic tips separately.

The optimality condition of a circumferential disc fin with nonuniform conduction and convection coefficients was discussed by Yu and Chen [40]. The nonlinear heat transfer equation for dry fins was solved by differential transformation and considered the fin-tip exposed in a convective-radiating environment. Lai et al. [41] divided a circumferential fin into numerous concentric circular sections. They assumed a nonuniform coefficient of convection and conduction while calculating the thermal performances of a dry annular fin. They demonstrated a recursive formulation for the adiabatic and diabetic fin-tip. Khani and Aziz [42] utilized a homotopy analysis to develop analytic solutions for longitudinal fins of the straight-narrow profile under the variability of conduction and convection. They validated their results by comparing them with those obtained by a numerical technique.

Kundu and Wongwises [43] analyzed a rectangular fin along with its primary surface, considering both convective and radiative heat exchange with the surroundings analytically. Adam et al. [44] summarized the results of the flow and heat transfer performance of compact fin-and-tube heat exchangers. Ghasemi et al. [45] used a differential transform method to analyze convective fins with temperature-dependent thermal conductivity and internal heat generation. Turkyilmazoglu [46] determined analytically thermal aspects of fins of exponential profile for temperature-dependent coefficients of the thermal conductivity and convection. A comparative study between exponential and straight fins was conducted by Turkyilmazoglu [47] for wet porous fins.

The main difficulty in analyzing fins is to consider the actual nature convection effect that creates the variability of the coefficient of convection. At the moistened fin surface, the mass transfer phenomenon also involves. The convection coefficients on the fin surface always vary due to the variety of events associated with the physical phenomena. The actual variations can have a temperature power law. The above literature survey shows that although there are plenty of investigations on the moistened fins, the researchers ignored

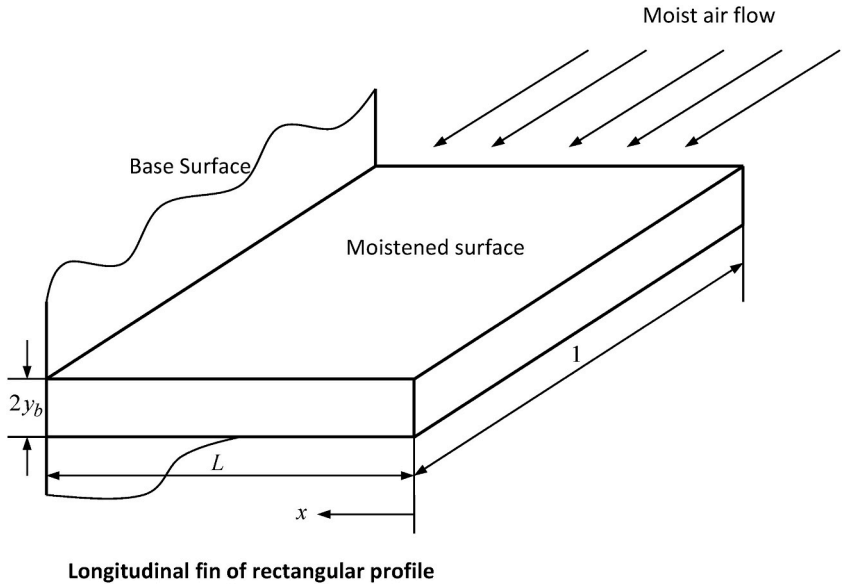

Fig. 1. Diagram of a moistened fin.

the combined effect of the polynomial connection between mass potential parameter and sensible potential heat transfer. Variable thermal conductivity, and variable convection coefficients have the emergence of nonlinearity in energy equation, which will be very difficult to handle analytically. A few works have been done but the actual design conditions were omitted. Thus, from the practical analysis aspect, those conditions are rarely favourable. On the other hand, using DTM to solve any nonlinear equation restricts the choice of the variable power factor as a positive integer [30]. The Adomian decomposition method, however, has no such limitation.

The present study implements an exact analytical technique to forecast the performance of rectangular-shaped moistened fins. It was well established that the thermal conductivity and convection always shows a variability nature for the fin design system. However, no work is available with these exact variations in moistened fins analytically. This investigation utilizes the dependability of thermal conductivity and any power-law type convection coefficients to take care of the actual variation. A power law-type mass transfer coefficient, along with a cubic algebraic expression between the absolute moisture content and the saturation temperature, is used to account for air dehumidification. The current analysis is uniformly suitable to any surface condition. The decomposition method is employed to analyze the design parameters of a moistened fin. The results were validated with the finite difference method. The present study provides the design information of moistened fins with the actual condition of surface heat transport. This analytical study's advantage is extending the optimization analysis for the highest heat load rate keeping a constraint volume to establish the superior design case. The effect of variable thermo-psychometric aspects shows significant dependability on the heat load transport process. The extremum heat transport rate and the design dimensions are predicted from the actual design implementation point of view. For the appropriate analytical method presented, the analysis can also be extended easily to a partially wet condition of a fin when both the dry and wet surface coexists during the dehumidification process.

2. Mathematical analysis

Fig. 1 shows schematically the geometrical parameters of a moistened fin having a uniform thickness. The sensible heat transfer may occur if the whole surface maintains above the saturation temperature. Otherwise, the fin turns into moistening, and the phenomena of mass diffusion exist. The heat transport mechanism is described above for the fin surface of different moistened conditions. The energy conservation law applied to an infinitesimally small control volume independent of time and condensation of moisture provides the following equations:

$$-\nabla \cdot \vec{q} = \frac{h}{y_b}(T - T_a) + \frac{h_m}{y_b}(\omega - \omega_a)h_{fg} \tag{1}$$

where, $\vec{q}$ is the conduction flux vector. The thermal conductivity is a variability parameter that is the sole function of temperature, $k = k_b[\,1 + \alpha\,(T - T_b)\,]$. Although Murray-Gardner's assumptions provide a solid ground for analyses of many fins, a few assumptions are gradually eliminated to have the real-life design situation. The heat and mass transfer coefficients vary for the variable resistance to heat transport along the fin surface. It has been shown by many researchers that the variability nature for the heat transfer coefficient in actual heat transport in fins can be fitted to a function of the power law $h = h_b\theta^m$. Here, m is the nonuniformity power factor and the appropriate magnitude of m can be estimated experimentally [48].

The dehumidification process involves the mass transport and also produces the energy transport. Chilton-Colburn analogy [49] makes a relationship between diffusion coefficients h and h_m as $h/h_m = c_p\,Le^{2/3}$. Solving Eq. (1) is impossible analytically as it has two dependent variables, T and ω. A very little moistened thickness is developed on the solid surface, and thus the thermal resistance of the condensate water layer can be assumed negligible. Therefore, the temperature of the condensate water can be considered equalized with the fin state potential level. The condensate water covers the solid surface with the saturation humid air and the psychrometric absolute moisture in the saturated air satisfies an algebraic expression of temperature only. The mathematical correlation between T and ω can be obtained from the air saturation properties. The absolute moisture content of humid air can be expressed as algebraic terms [50] by applying the best fit method without losing any generality as

$$\omega = A + BT + CT^2 + DT^3 \tag{2}$$

where

$$\begin{bmatrix} A \\ B \\ C \\ D \end{bmatrix} = \begin{bmatrix} 3.7444 \times 10^{-3} \\ 0.3078 \times 10^{-3}\ {}^0C^{-1} \\ 0.0046 \times 10^{-3}\ {}^0C^{-2} \\ 0.0004 \times 10^{-3}\ {}^0C^{-3} \end{bmatrix} \tag{3}$$

Eqs. (1) and (2) are used to form the heat transport equation for thin moistened fins for transport processes, and it can be delineated in a normalized form as

$$(1+\beta)\frac{d^2\theta}{dX^2} - \beta\,\theta\frac{d^2\theta}{dX^2} - \beta\left(\frac{d\theta}{dX}\right)^2 - \delta_0\theta^m - \delta_1\theta^{m+1} - \delta_2\theta^{m+2} - \delta_3\theta^{m+3} = 0 \tag{4}$$

where

$$\begin{bmatrix}\delta_0\\ \delta_1\\ \delta_2\\ \delta_3\end{bmatrix}=\begin{bmatrix}Z_0^2\xi\left(\omega_a-A-BT_a-CT_a^2-DT_a^3\right)/\left(T_a-T_b\right)\\ Z_0^2+Z_0^2\xi\left(B+2CT_a+3DT_a^2\right)\\ -Z_0^2\xi\left(C+3DT_a\right)\left(T_a-T_b\right)\\ Z_0^2\xi\, D(T_a-T_b)^2\end{bmatrix} \tag{5}$$

$$\begin{bmatrix}X\\ Z_0\\ \psi\end{bmatrix}=\begin{bmatrix}x/L\\ \sqrt{Bi}/\psi\\ y_b/L\end{bmatrix} \tag{6}$$

and

$$\begin{bmatrix}Bi\\ \beta\\ \xi\\ \theta\end{bmatrix}=\begin{bmatrix}h_b y_b/k_b\\ \alpha\left(T_a-T_b\right)\\ h_{fg}/c_p\, Le^{2/3}\\ (T_a-T)/(T_a-T_b)\end{bmatrix} \tag{7}$$

Eq. (4) is solved by the Adomian decomposition method (ADM). Mathematical expressions for energy transfer at the boundary are taken as,

$$\text{at } X=0,\ d\theta/dX=0 \tag{8}$$

$$\text{at } X=1,\ \theta=1 \tag{9}$$

Here, it is to describe that the thermal pattern in moistened fins depends naturally on the tip condition. As the tip surface exposes to the moist air to be cooled, heat and mass transport at the tip surface occurs due to potentiality factors present. However, these potentialities are generally too small to transport a significant amount of heat. Due to this reason, the insulated condition can generally be adopted to avoid a complicated analysis without much error associated with the study [1]. On the other hand, there is always possibility to improve the analysis based on the insulated tip condition for the exchange of heat through the tip surface by assuming the fin length equal to the actual fin length plus half-thickness of the fin hypothetically. This design consideration improves the analysis with the convected tip. In contrast a separate analysis is not required by including the heat exchange at the tip surface for the accurate study. Due to this practical reason, the insulated tip has been employed to establish the present ADM model.

The purpose and suitability of applying ADM in this investigation were originally described by George Adomian in his pioneering work in 1988 [51]. The ADM is an approximation and it is an infinite series. Actually, an accurate solution is often obtained by employing this method for a very small value of n as it provides rapidly convergent series. To apply ADM, one can write Eq. (4) as,

$$\frac{d^2\theta}{dX^2}-\frac{\beta}{(1+\beta)}\theta\frac{d^2\theta}{dX^2}-\frac{\beta}{(1+\beta)}\left(\frac{d\theta}{dX}\right)^2-K_0\theta^m-K_1\theta^{m+1}-K_2\theta^{m+2}-K_3\theta^{m+3}=0 \tag{10}$$

where

$$K_j=\delta_j\,/\,(1+\beta);\ j=0,1,2,3 \tag{11}$$

The principal algorithm of ADM [51] is described below for solving Eq. (10):

$$\Delta\theta=\frac{\beta}{(1+\beta)}NA+\frac{\beta}{(1+\beta)}NB+K_0NC+K_1ND+K_2NE+K_3NF \tag{12}$$

where Δ is the maximum order derivative and it is second-order in this case. The inverse of Δ is

$$\Delta^{-1}(\bullet)=\int_0^X\int_0^X(\bullet)\,dX\,dX \text{ for } (0\le X\le 1) \tag{13}$$

and the nonlinear terms are

$$NA=\theta\frac{d^2\theta}{dX^2}=\sum_{n=0}^{\infty}A_n;\ NB=\left(\frac{d\theta}{dX}\right)^2=\sum_{n=0}^{\infty}B_n;\ NC=\theta^m=\sum_{n=0}^{\infty}C_n;\ ND=\theta^{m+1}=\sum_{n=0}^{\infty}D_n;NE=\theta^{m+2}=\sum_{n=0}^{\infty}E_n;\ NF=\theta^{m+3}=\sum_{n=0}^{\infty}F_n \tag{14}$$

The Adomian polynomials were explained in Ref. [51]. As Δ is an operator of second order, Δ^{-1} is a double integral.

$$\Delta^{-1}\Delta\theta=\theta(X)-\theta(0)-Xd\theta(0)\,/\,dX\ (\,0\le X\le 1) \tag{15}$$

Multiplying Δ^{-1} on both sides of Eq. (12) which yields,

$$\Delta^{-1}\Delta\theta = \frac{\beta}{(1+\beta)}\Delta^{-1}\left(\theta\frac{d^2\theta}{dX^2}\right) + \frac{\beta}{(1+\beta)}\Delta^{-1}\left(\frac{d\theta}{dX}\right)^2 + K_0\,\Delta^{-1}\left(\theta^m\right) + K_1\,\Delta^{-1}\left(\theta^{m+1}\right) + K_2\,\Delta^{-1}\left(\theta^{m+2}\right) + K_3\,\Delta^{-1}\left(\theta^{m+3}\right)\ (\,0 \le X \le 1) \tag{16}$$

Using Eq. (15), Eq. (16) can be written as

$$\theta = \theta(0) + Xd\theta(0)\,/\,dX + \Delta^{-1}(NA) + \Delta^{-1}(NB) + \Delta^{-1}(NC) + \Delta^{-1}(ND) + \Delta^{-1}(NE) + \Delta^{-1}(NF)\ (\,0 \le X \le 1) \tag{17}$$

The Adomian decomposition method provides the temperature response obtained from Eq. (17), which is convergent infinite series,

$$\theta = \sum_{n=0}^{\infty}\theta_n \tag{18}$$

Using Eqs. (8) and (18), Eq. (17) becomes as

$$\sum_{n=0}^{\infty}\theta_n(X) = \theta_t + \frac{\beta}{(1+\beta)}\sum_{n=0}^{\infty}A_n + \frac{\beta}{(1+\beta)}\sum_{n=0}^{\infty}B_n + \sum_{n=0}^{\infty}C_n + \sum_{n=0}^{\infty}D_n + \sum_{n=0}^{\infty}E_n + \sum_{n=0}^{\infty}F_n\ (\,0 \le X \le 1) \tag{19}$$

The tip temperature $\theta(0)$ is denoted as θ_t. The matrix form of Eq. (19) can be written as,

$$\begin{bmatrix}\theta_1\\ \theta_2\\ \theta_3\\ \vdots\end{bmatrix} = \begin{bmatrix}\frac{\beta}{(1+\beta)}\Delta^{-1}(A_0) + \frac{\beta}{(1+\beta)}\Delta^{-1}(B_0) + \Delta^{-1}(C_0) + \Delta^{-1}(D_0) + \Delta^{-1}(E_0) + \Delta^{-1}(F_0)\\ \frac{\beta}{(1+\beta)}\Delta^{-1}(A_1) + \frac{\beta}{(1+\beta)}\Delta^{-1}(B_1) + \Delta^{-1}(C_1) + \Delta^{-1}(D_1) + \Delta^{-1}(E_1) + \Delta^{-1}(F_1)\\ \frac{\beta}{(1+\beta)}\Delta^{-1}(A_2) + \frac{\beta}{(1+\beta)}\Delta^{-1}(B_2) + \Delta^{-1}(C_2) + \Delta^{-1}(D_2) + \Delta^{-1}(E_2) + \Delta^{-1}(F_2)\\ \vdots\end{bmatrix} \tag{20}$$

where A_n, B_n, C_n, D_n, E_n, and F_n are Adomian polynomials. The solution is associated with the n-term approximation. Only a small number of terms are necessary for the mathematical expressions because of the rapidity of the convergence for the Adomian decomposition method.

$$\begin{bmatrix}\theta_1\\ \theta_2\\ \theta_3\\ \theta_4\\ \vdots\end{bmatrix} = \begin{bmatrix}w_0X^2/2\,!\\ w_1X^2/2\,! + w_2X^4/4\,!\\ w_3X^2/2\,! + w_4X^4/4\,! + w_5X^6/6\,!\\ w_6X^2/2\,! + w_7X^4/4\,! + w_8X^6/6\,! + w_9X^8/8\,!\\ \vdots\end{bmatrix} \tag{21}$$

where

$$\begin{bmatrix}w_0\\ w_1\\ w_2\\ w_3\\ w_4\end{bmatrix} = \begin{bmatrix}\sum_{n=0}^{3}K_n\,\theta_t^{m+n}\\ \beta\,w_0\,\theta_t/(1+\beta)\\ w_0\sum_{n=0}^{3}(m+n)K_n\,\theta_t^{m+n-1}\\ \beta\,w_1\,\theta_t/(1+\beta)\\ \beta\left(w_2\theta_t + 3w_0^2\right)\Big/(1+\beta) + w_1\sum_{n=0}^{3}(m+n)K_n\,\theta_t^{m+n-1}\end{bmatrix} \tag{22}$$

and

$$\begin{bmatrix}w_5\\ w_6\\ w_7\\ w_8\\ w_9\end{bmatrix} = \begin{bmatrix}w_2\sum_{n=0}^{3}(m+n)K_n\theta_t^{m+n-1} + 3w_0^2\sum_{n=0}^{3}(m+n)\,(m+n-1)\,K_n\theta_t^{m+n-2}\\ \beta w_3\theta_t/(1+\beta)\\ \beta(6w_0w_1 + w_4\theta_t)/(1+\beta) + w_3\sum_{n=0}^{3}(m+n)K_n\theta_t^{m+n-1}\\ \beta(15w_0w_2 + w_5\theta_t)/(1+\beta) + w_4\sum_{n=0}^{3}K_n(m+n)\theta_t^{m+n-1} + 6w_0w_1\sum_{n=0}^{3}K_n(m+n)\,(m+n-1)\theta_t^{m+n-2}\\ w_5\sum_{n=0}^{3}(m+n)K_n\theta_t^{m+n-1} + 15w_0w_1\sum_{n=0}^{3}(m+n)\,(m+n-1)K_n\theta_t^{m+n-2} + 15w_0^3\sum_{n=0}^{3}(m+n)\,(m+n-1)\,(m+n-2)K_n\theta_t^{m+n-3}\end{bmatrix} \tag{23}$$

The solution for the thermal state of a moistened fin is obtained from Eqs. (18), (21) and (23) which is a convergent series. One can write the thermal response as

$$\theta = (w_0 + w_1 + w_3 + w_6)\frac{X^2}{2!} + (w_2 + w_4 + w_7)\frac{X^4}{4!} + (w_5 + w_8)\frac{X^6}{6!} + w_9\frac{X^8}{8!} + \cdots \tag{24}$$

The temperature distribution expressed in Eq. (24) is utilized after knowing the tip state temperature θ_t. It can be determined using the base condition delineated in Eq. (9). A flow chart of the proposed semi-analytical scheme for determining the fin temperature comprising the steps regarding ADM is shown in Fig. 2.

From the thermal state condition, the actual energy transport per unit width from a moistened fin is readily normalized by utilizing the gradient approach at the base as

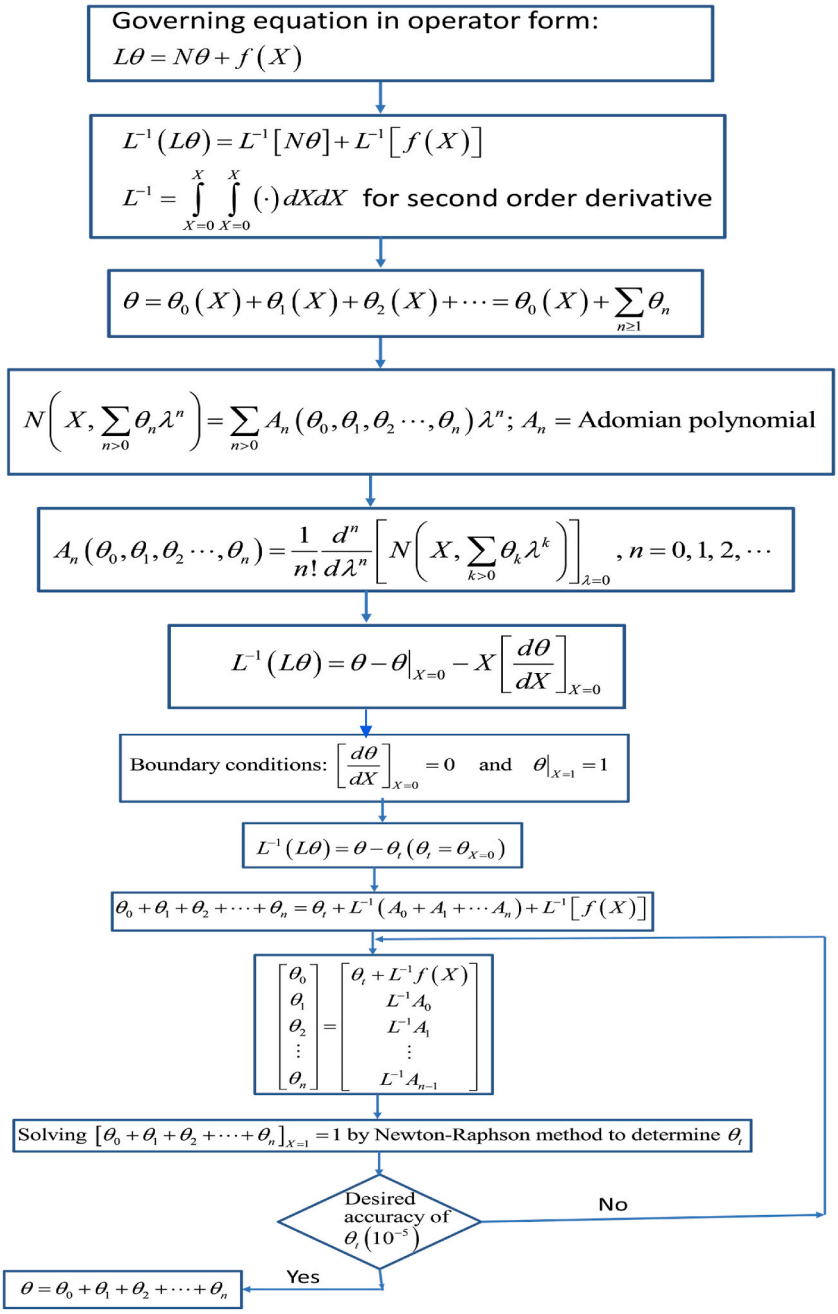

Fig. 2. Flow chart of Adomian decomposition method used in this study.

$$Q=\frac{q}{2k_b(T_a-T_b)}=\psi\left[(w_0+w_1+w_3+w_6)+\frac{1}{3!}(w_2+w_4+w_7)+\frac{1}{5!}(w_5+w_8)+\frac{1}{7!}w_9+\cdots\right] \tag{25}$$

The maximum possible heat load rate from a moistened fin can be normalized as

$$Q_i=\frac{q_i}{2k_b(T_a-T_b)}=\psi\sum_{n=0}^{3}\delta_n \tag{26}$$

2.1. Fin performance parameters

One can write the moistened efficiency η for transporting heat in a fin as,

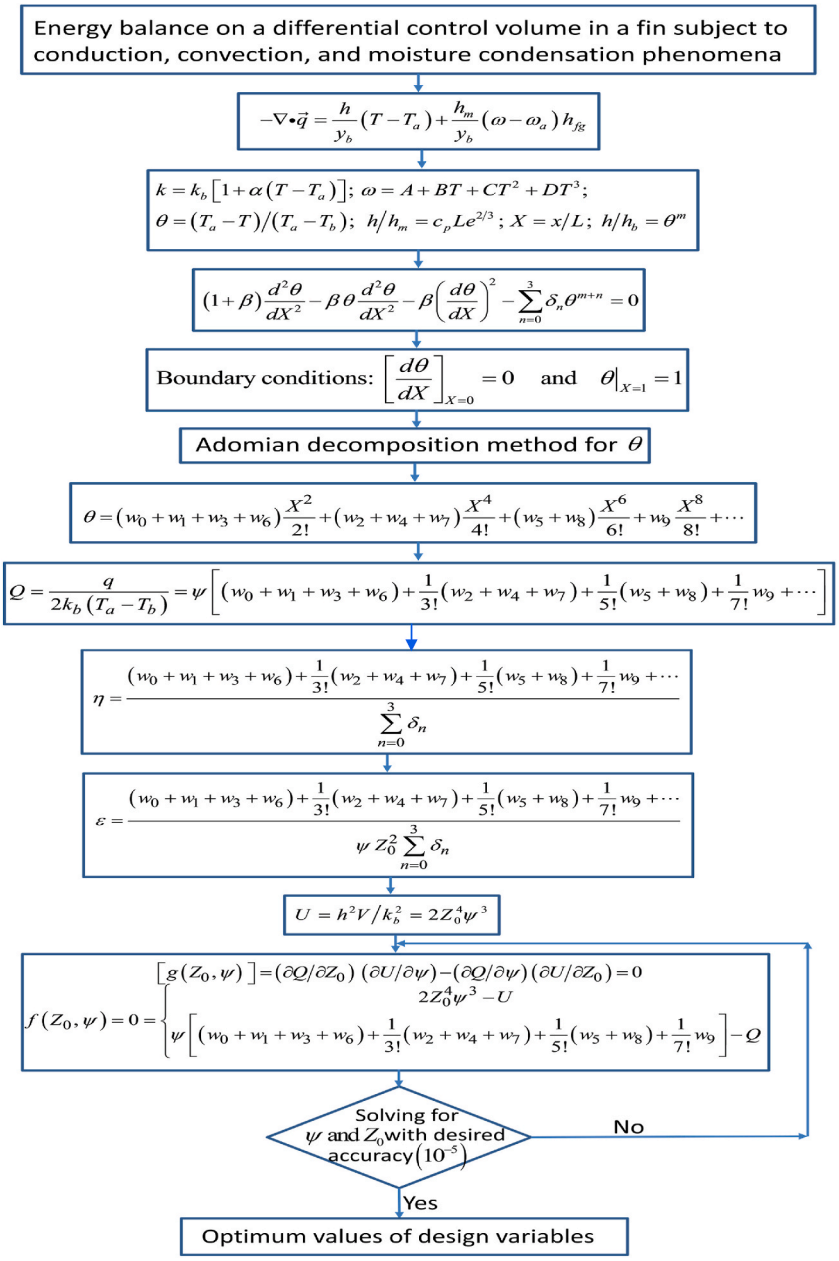

Fig. 3. Flow chart of the proposed mathematical model.

$$\eta=\frac{Q}{Q_i}=\frac{(w_0+w_1+w_3+w_6)+\frac{1}{3!}(w_2+w_4+w_7)+\frac{1}{5!}(w_5+w_8)+\frac{1}{7!}w_9+\cdots}{\sum_{n=0}^{3}\delta_n} \tag{27}$$

One can express the moistened fin effectiveness ε as,

$$\varepsilon=\frac{(w_0+w_1+w_3+w_6)+\frac{1}{3!}(w_2+w_4+w_7)+\frac{1}{5!}(w_5+w_8)+\frac{1}{7!}w_9+\cdots}{\psi\, Z_0^2\sum_{n=0}^{3}\delta_n} \tag{28}$$

2.2. Extremum design aspects

An efficient thermal system must design a fin shape to accomplish the highest rate of energy transport subject to constraint design conditions and provide a wide-ranging guideline to evaluate the normalized characteristic features of a well-designed fin. Fin extremum design can be carried out by considering different design situations. In this investigation, the optimization is studied by establishing the optimality criteria to evaluate the appropriate dimensions of a moistened fin for practical applications.

A system is developed for designing a rectangular longitudinal fin in wet conditions with all non-linear effects for the heat transport mechanism. The geometrical volume of a moistened fin having the width of unity is normalized as,

$$U=h^2V/k_b^2=2Z_0^4\psi^3 \tag{29}$$

For wet fins with the constant thermo-psychrometric parameters, Z_0 and ψ are connecting with Q and U. From the single-objective optimization analysis, the condition of the extremum equation is derived as,

$$[g(Z_0,\psi)\,]=(\partial Q/\partial Z_0)\,(\partial U/\partial\psi)-(\partial Q/\partial\psi)\;\;(\partial U/\partial Z_0)=0 \tag{30}$$

Utilizing Eqs. (25) and (29), Eq. (30) converts into the following equation as

$$\begin{aligned} g(Z_0,\psi)=\;&3Z_0\left(\frac{\partial w_0}{\partial Z_0}+\frac{\partial w_1}{\partial Z_0}+\frac{\partial w_3}{\partial Z_0}+\frac{\partial w_6}{\partial Z_0}\right)+\frac{Z_0}{2}\left(\frac{\partial w_2}{\partial Z_0}+\frac{\partial w_4}{\partial Z_0}+\frac{\partial w_7}{\partial Z_0}\right)+\frac{Z_0}{40}\left(\frac{\partial w_5}{\partial Z_0}+\frac{\partial w_8}{\partial Z_0}\right)+\frac{3Z_0}{7!}\frac{\partial w_9}{\partial Z_0}\\ &-4\left(w_0+w_1+w_3+w_6+\psi\frac{\partial w_0}{\partial\psi}+\psi\frac{\partial w_1}{\partial\psi}+\psi\frac{\partial w_3}{\partial\psi}+\psi\frac{\partial w_6}{\partial\psi}\right)-\frac{2}{3}\left(w_2+w_4+w_7+\psi\frac{\partial w_2}{\partial\psi}+\psi\frac{\partial w_4}{\partial\psi}+\psi\frac{\partial w_7}{\partial\psi}\right)\\ &-\frac{1}{30}\left(w_5+w_8+\psi\frac{\partial w_5}{\partial\psi}+\psi\frac{\partial w_8}{\partial\psi}\right)-\frac{4}{7!}\left(w_9+\psi\frac{\partial w_9}{\partial\psi}\right)=0 \end{aligned} \tag{31}$$

For the extremum condition, Eq. (31) has been solved. However, it has two unknown variables Z_0 and ψ, and thus another constraint equation is needed for the solution process. A generalized model is developed such that one can use any one of the two as a design constraint (either U or Q). With this logic, the constraint equation can be constructed as,

$$f(Z_0,\psi)=0=\begin{cases} 2Z_0^4\psi^3-U \\ \psi\left[(w_0+w_1+w_3+w_6)+\dfrac{1}{3!}(w_2+w_4+w_7)+\dfrac{1}{5!}(w_5+w_8)+\dfrac{1}{7!}w_9\right]-Q \end{cases} \tag{32}$$

Eqs. (31) and (32), being transcendental and non-homogeneous, have been solved together by a numerical approach determining the design values of Z_0 and ψ. The Newton-Raphson iterative method can be engaged in the process of the solution for calculating the roots of these equations to establish an extremum condition. For each iteration, the following sufficient conditions are to be satisfied in computations towards the final solution for the desired roots:

$$J\left[f\frac{\partial^2 g}{\partial Z_0\partial\psi}-g\frac{\partial^2 f}{\partial Z_0\partial\psi}-\left(\frac{\partial g}{\partial Z_0}\right)\left(\frac{\partial f}{\partial\psi}\right)+\left(\frac{\partial f}{\partial Z_0}\right)\left(\frac{\partial g}{\partial\psi}\right)\right]+\frac{\partial J}{\partial Z_0}\left(g\frac{\partial f}{\partial\psi}-f\frac{\partial g}{\partial\psi}\right)>0 \tag{33}$$

and

$$J\left[g\frac{\partial^2 f}{\partial Z_0\partial\psi}-f\frac{\partial^2 g}{\partial Z_0\partial\psi}-\left(\frac{\partial f}{\partial Z_0}\right)\left(\frac{\partial g}{\partial\psi}\right)+\left(\frac{\partial f}{\partial\psi}\right)\left(\frac{\partial g}{\partial Z_0}\right)\right]+\frac{\partial J}{\partial\psi}\left(f\frac{\partial g}{\partial Z_0}-g\frac{\partial f}{\partial Z_0}\right)>0 \tag{34}$$

where J is the Jacobian determinant which is

$$J=\begin{vmatrix}\partial f/\partial Z_0 & \partial f/\partial\psi\\ \partial g/\partial Z_0 & \partial g/\partial\psi\end{vmatrix} \tag{35}$$

The final roots of ψ and Z_0 are predicted until they satisfy a necessary condition of the convergence. This condition can be set on the basis of the requirement of the accuracy level. In this work, the difference value of the magnitude between two successive iterations for any root was less than and equal to10^{-5} to yield the optimum value. Fig. 3 shows the flow chart of the proposed mathematical model.

3. Results and discussion

The humid air cools at the fin surface and becomes saturated, and its thermal state changes in the energy transport direction. The psychometric state points of moist air are a design constant, and the results have been taken with a constant surrounding pressure (1.0132 bar). The initial aim of the current study is to authenticate results before presenting them and it can be carried out with the help of numerical results. The governing equation involved in the present study can be solved using the finite difference scheme with the boundary conditions associated with the analysis. To perform this task, finalizing the total number of grids (grid-independent test) is required to be fixed to produce correct results. This observation can be examined by considering 76, 101, and 126 lattice points. A marginal variation is noticed (less than 0.05%) when results are generated with 101 and 126 lattice points, and thus, the present numerical results are taken with 101 grid points.

Another way to validate the present analysis is by omitting the mass transfer effect and non-variability of thermo-physical parameters. With these design situations, the temperature can be predicted by a closed-form solution quickly. Fig. 4 depicts the thermal history in a moistened fin evaluated by this work for the exact analysis (simplified case) and the numerical analysis. This study shows that the present model matches the simplified case used to determine the temperature state analytically. The graphs are drawn for different fin parameter (Z_0) values. The current analytical and numerical results of the moistened fin for all non-linearities are drawn in Fig. 4b. An excellent agreement of results was found. Hence, the present ADM model using is well suited for any class of moistened fin equations. A comparison of these two figures highlights that the normalized temperature of moistened fins always diminishes for the actual design condition compared to the ideal theoretical value. Further, Table 1 shows a comparative study between the proposed ADM and the numerical scheme based on the finite difference method. The temperature distribution predicted by the above techniques shown has an insignificant deviation. This comparative study also highlights that the proposed method has no limitation to solving the heat conduction equation of moistened fins with the variation of any fractional power law of heat and mass transfer coefficients to be applicable in actual cases.

The psychrometric property of humidity (relative) of the surrounding wind on the thermal state level in moistened fins is presented in Fig. 5a. It can be evident from the figure that this humid air property is a big responsibility for the temperature pattern. Higher moisture always increases the surface temperature of moist fins by releasing extra latent energy. The results have been plotted for nonuniformities of the coefficient of diffusion events. The fin temperature field affected by relative humidity in the actual condition of the moistened fin surface can be studied from this diagram. Fig. 5b depicts the dependability of the variability effect of coefficients of heat and mass transport on the temperature pattern and shows a significant change. The experimental methods may be necessary to ascertain the actual change in the convection coefficients [52,53]. Fig. 5b can compare the thermal state level of a moistened fin for uniform and nonuniform heat and mass transfer coefficients. Due to the increase in surface resistance, the variable nature of heat and mass transfer coefficients induces an enhancement in fin temperature. The dependency index factor m is taken as 0, 1, 2, and 3 for plotting, and $m = 0$ implies the uniformity condition of the heat and mass transfer coefficients and provides the minimum thermal temperature level variation in the fin. Under this design situation, thermal resistance to heat flow in the moistened fin is significantly low. In the actual application, the index of the variability coefficient m depends on the design condition. However, the present model is equally suitable at any value of m to be considered based on the design aspect. Therefore, this study is so essential to implement the practical case study. Fig. 5c is plotted for the impact of non-uniformity of the thermal conduction coefficient on developing the thermal field in the case of the moistened surface. As β increases within the practical value, the temperature state level of the moistened fin decreases by diminishing the conductive resistance, which is an expected trend from the physical standpoint. But it is also apparent that this diagram shows the non-dominant effect of non-uniformity of the thermal conductivity on the moistening temperature level.

The heat transport performances are regarded as important characteristics of fins; hence, they are estimated at a design circumstance. To satisfy this aspect, the moistening performance indices for dry and wetted surfaces are demonstrated by the present and exact analytical models. Energy transport performances are plotted against Z_0, a design variable to show the effects of different parameters, like RH and m. Fig. 6a is plotted for the efficiency of the dry fin surface with the varying m and the validation is done for the curve by omitting the non-linearity effect. Fig. 6b depicts the effectiveness with the same condition as in the previous figure. The fin performances have been shown pronounced effects on the variability of the heat and mass transfer coefficient factors. A positive m continuously decreases moistened fin performances for the increase in temperature state points variation attributed to the fin. For the

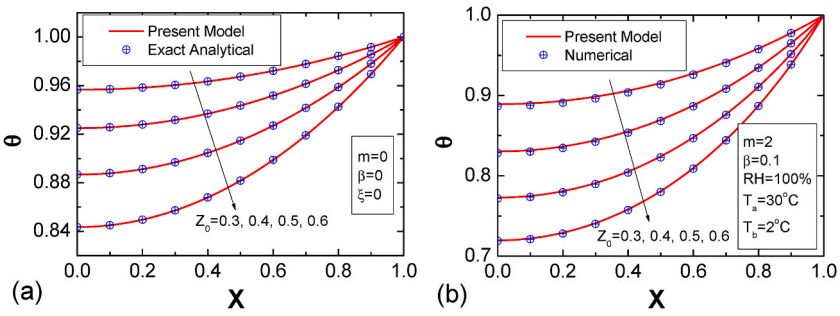

Fig. 4. Validation of present analysis by comparing temperature distributions determined using exact analytical and numerical analyses: (a) Dry surface with ideal condition and (b) Wet surface with all non-linearity effects.

Table 1
Temperature distribution in a wet fin predicted by the present analysis and a finite difference method for a design condition, $m = 3.5$, $Z_0 = 0.5$, $\beta = 0.01$, $T_a = 30^oC$, $T_b = 2^oC$, and $RH = 90\%$.

X	θ		Deviation $\frac{\lvert P_1 - P_2 \rvert}{P_1} \times 100$
	Present analysis (P1)	Finite difference method (P2)	
0.00	0.8172653	0.8158429	0.1740
0.05	0.8176583	0.8161700	0.1820
0.10	0.8188389	0.8173035	0.1875
0.15	0.8208119	0.8192477	0.1906
0.20	0.8235855	0.8220101	0.1913
0.25	0.8271710	0.8256014	0.1897
0.30	0.8315836	0.8300357	0.1861
0.35	0.8368419	0.8353311	0.1805
0.40	0.8429687	0.8415091	0.1731
0.45	0.8499912	0.8485958	0.1642
0.50	0.8579410	0.8566220	0.1537
0.55	0.8668552	0.8656234	0.1421
0.60	0.8767763	0.8756415	0.1294
0.65	0.8877534	0.8867246	0.1159
0.70	0.8998426	0.8989278	0.1017
0.75	0.9131076	0.9123150	0.0868
0.80	0.9276216	0.9269593	0.0714
0.85	0.9434671	0.9429450	0.0553
0.90	0.9607385	0.9603693	0.0384
0.95	0.9795424	0.9793443	0.0202
1.00	1.0000000	1.0000000	0.0000

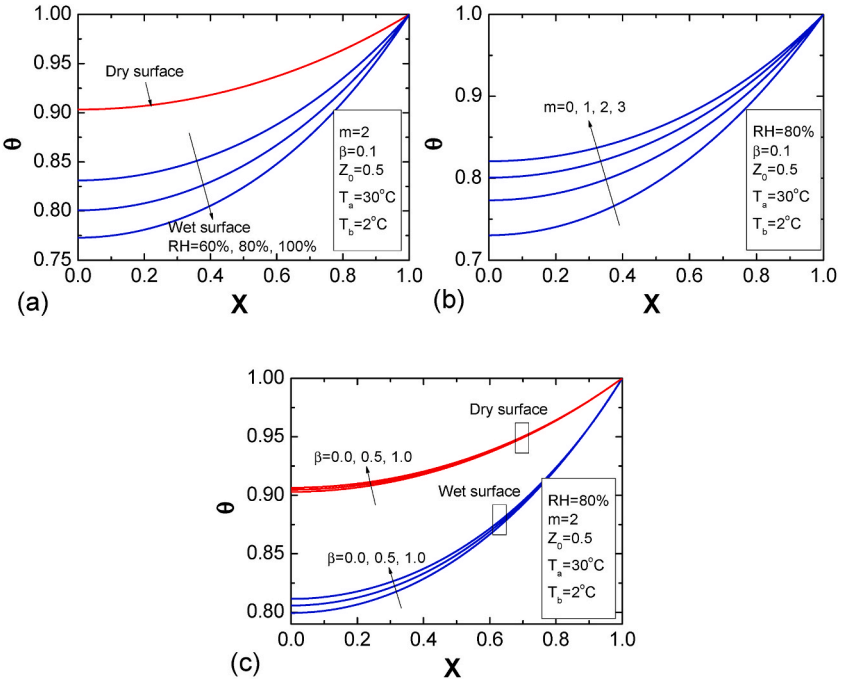

Fig. 5. Fin surface temperature as a function of relative humidity, variable convective coefficient parameter, and variable conductivity: (a) Influence of relative humidity, (b) Effect of m, and (c) Effect of β.

comparison of the current and published models, Table 2 has been constructed to show the correctness of the proposed model with the heat and mass transfer coefficients correlated with temperature as an integer power law taken due to the limitation of the differential transform method established in the previous work [54]. Under a common design condition, the present model predicted the fin efficiency with high accuracy as values coincide with the published results according to this Table.

The design effect of changing heat and mass transfer coefficients upon moistened fin efficiency and effectiveness has been studied in Fig. 7a and b, for wet surface conditions. The performances with a constant convection parameter are also drawn in this figure for comparison. It can be noticed that both the moistening performance parameters decrease appreciably with an increasing power index of m. The coefficients of convective heat and mass transfer alter for the non-uniformity boundary layer thicknesses produced,

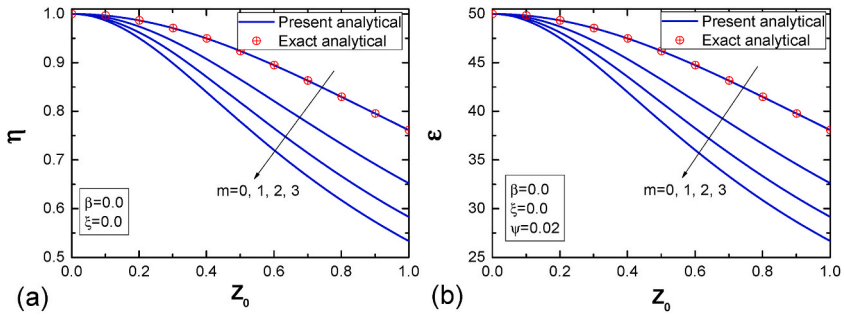

Fig. 6. Comparisons of present and exact analytical model with variability effect of coefficient of convection: (a) Fin efficiency and (b) Fin effectiveness.

Table 2
Comparison of efficiency of wet fins evaluated by the present study and published work [54] at $T_a = 30^oC$, $T_b = 2^oC$, $m = 2$, and $\beta = 0.01$.

Z_0	Efficiency, η	
	Present	Published
0.00001	1.0000000	1.0000000
0.05	0.9931849	0.9931593
0.10	0.9735763	0.9734798
0.15	0.9434041	0.9432066
0.20	0.9056236	0.9053129
0.25	0.8632190	0.8627978
0.30	0.8187359	0.8182165
0.35	0.7740950	0.7734942
0.40	0.7306054	0.7299408
0.45	0.6890731	0.6883612
0.50	0.6499323	0.6491874
0.55	0.6133620	0.6125957
0.60	0.5793765	0.5785984
0.65	0.5478908	0.5471082
0.70	0.5187646	0.5179833
0.75	0.4918315	0.4910557
0.80	0.4669166	0.4661494
0.85	0.4438476	0.4430914
0.90	0.4224611	0.4217174
0.95	0.4026053	0.4018753
1.00	0.3841414	0.3834256

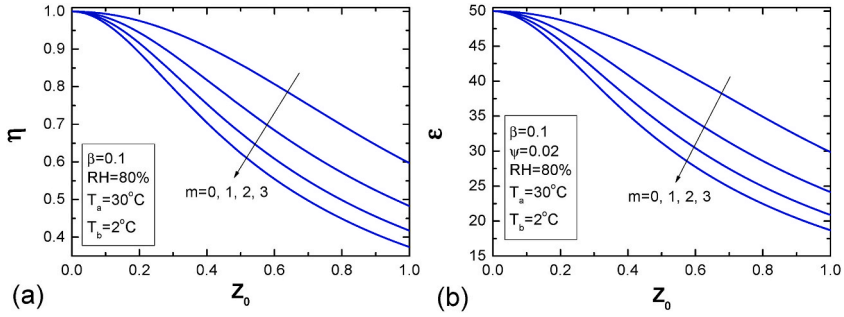

Fig. 7. Effect of variable convection parameter and thermal parameter Z_0 on moisten fin performances: (a) Fin efficiency and (b) Fin effectiveness.

increasing the resistance to energy flow and, in turn, decreasing heat transport performances. It can be highlighted that the convection coefficients decrease in an increase in fin temperature direction, and this effect can be included by considering a positive m value. Thus, considering the actual condition at the fin surface, fin performances are always lesser values clearly shown in these figures.

In Fig. 8a, the energy transport performance dependent on RH is established for the actual condition for heat transfer load from the moistened surface. Variations are plotted in the same diagram for both dry and moist surfaces. From the η vs. Z_0 graph, it is evident that the moistened air significantly declines efficiency. The plot shows a weak connection between fin efficiency and relative humidity. In cooling systems, a dehumidifying process occurs adjoining the heat transfer surface when it is below the saturation value. Saturation temperature correlates with the psychometric state. However, for the actual study, the fin efficiency changes slowly with the relative

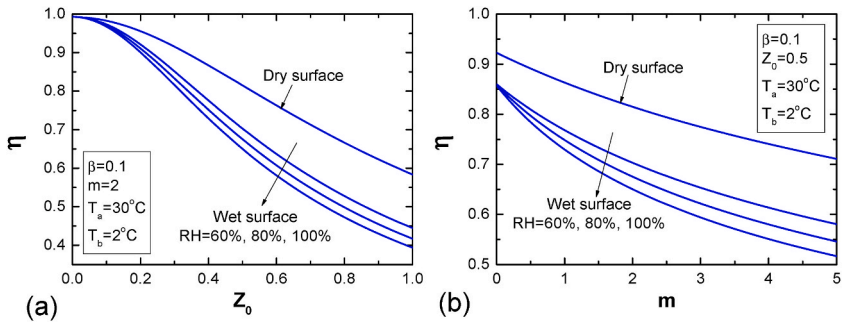

Fig. 8. Fin efficiency dependent function of different design parameters: (a) Fin parameter Z_0 and (b) Power index of convection coefficient m.

humidity. Fig. 8b is plotted to determine the connectivity function between the fin performance and variability factor of the convection parameter m for different surface conditions. It is noted that the design index m declines the heat transfer performance. This reduction is relatively more for the design of moist surfaces and the greatest variation is observed at 100% RH. This trend is due to the condensation effect, which is a maximum at that RH. Under this design condition, there is the highest fin surface temperature. The convection coefficient variability reduces the fin efficiency's maximum effect at 100% RH. From this graph, it is crucial that the moistened fin efficiency can be determined directly at any value of surface heat coefficient m from 0 to 5 without any calculation. Thus, this graph may be helpful to a designer for determining the fin efficiency in dehumidifying conditions for the actual case study application where known design aspects are specified.

The fin surface maintains below the surrounding temperature in refrigeration and air conditioning applications where moist air strikes this surface and is required to cool. This circumstance involves the heat and mass transfer on the solid surface for the difference of the temperature and specific humidity. The non-uniform heat and mass transfer coefficients along the conduction direction in a fin are due to the variable thickness of the boundary layers. In the present study, the above effects have been taken care of by choosing uneven heat and mass transfer coefficients as a temperature power law. An experiment can determine the values of power factors, and the fractional power factor would be applicable in actual cusses. However, developing the proposed model based on the Adomian decomposition method with any integer or fractional power factors is no limitation. But the differential transform method or other procedures will have restrictions in choosing the fractional power law. Table 3 is prepared for the above comments highlighting surface conditions' effect on fins' heat transfer. The moistened fin has always transferred more heat than the dry surface fin to release latent heat at the solid-air interface, as illustrated in this Table. This influence dominates with the air's moisture content increase by amplifying the relative humidity. The actual case study at a high m always declines the fin's energy transfer ability.

The Biot number (Bi) plays a significant role in conducting heat in solids. Fig. 9a depicts the effect of Bi on heat load transferred in a moist fin with different moisture contents of humid air for unfaltering fin volume. For different relative humidity of surrounding air, incremented Bi initially enhances the energy transfer through a fin; it becomes the highest value, then declines rather slowly. The extremer situation is shown corresponding to the highest heat transfer rates. It can be observed from the graph that the trend for different moistened surface conditions is similar, and the design Biot number and highest heat transfer rate relate almost a linear function. This diagram shows that the relative humidity amplifies the design Bi to satisfy the least resistance under a practical condition. Fig. 9b shows the heat transfer duty through a moistened fin, varying Bi with different normalized volumes. As the normalized volume amplifies, predictably, the heat load also enhances. For a particular U, the highest heat load is possible for a specific Bi which corresponds to the thermo-geometric parameter of the moistened fin. Fig. 7c shows an exact trend of the fin performance with the design Bi for different constant fin volumes. An increase in efficiency does not ensure the maximum enhancement in heat transfer rate. The fin performance at the extremum design situation doesn't satisfy either the highest or the lowest. For a lower value of Bi, the curve is steeper. With all non-linearity effects, the efficiency values are more or less 60% for the maximum heat transfer rates. Therefore, from the design point of view, this information may also help in choosing a fin for enhancing the heat transfer load.

Then, an effort was employed to draw the design curves for predicting the unknown design variables from the graph. Fig. 10a shows the variation of the maximum heat transfer from moistened fins for a unique range of normalized fin volume. Optimum Bi in dehumidification processes is drawn with the normalized fin volume in Fig. 10b. Graphs are constructed for different RH values for wet surfaces and for dry surfaces to maintain an experimental condition. The optimum normalized heat load initially increases rapidly with the amplifying volume; then, the increment gradually slows down. At an unvarying fin volume, amplifying the design value of Bi provides the highest heat transfer rate achieved with an incremented relative humidity. Fig. 10a and b can be utilized jointly to treat the design plot for the rectangular-shaped moistened fin considering all non-linearity effects. To implement a design case with known variables Q, psychometric properties of humid air, and primary surface temperature, values of m and β are known, and the required normalized fin volume can be determined from Fig. 10a. Now utilizing this volume at the extremum condition, Bi can be traced from Fig. 10b. Then, the aspect ratio ψ is obtained from the mathematical expression of the volume. Therefore, all the unknowns at an optimum design can be determined from the design curves. And hence, the design curves assist in avoiding the extensive numerical process required in the present model to obtain unknown design parameters.

Table 3
Dimensionless heat transfer rate for dry and wet surfaces of a fin dependent on variable convective coefficients at $\beta = 0.01$, $Z_0 = 0.5$, $\psi = 0.05$, $T_b = 2\,^oC$, and $T_a = 30\,^oC$.

m	Q				
	Wet surface				Dry surface
	RH = 70%	RH = 80%	RH = 90%	RH = 100%	
0.00	0.0256711	0.0284787	0.0312943	0.0341195	0 .0115532
0.25	0.0247896	0.0273928	0.0299819	0.0325582	0.0113543
0.50	0.0240076	0.0264428	0.0288496	0.0312301	0.0111672
0.75	0.0233061	0.0255998	0.0278559	0.0300770	0.0109907
1.00	0.0226707	0.0248432	0.0269718	0.0290598	0.0108236
1.25	0.0220908	0.0241579	0.0261768	0.0281513	0.0106652
1.50	0.0215580	0.0235323	0.0254554	0.0273315	0.0105145
1.75	0.0210657	0.0229575	0.0247958	0.0265856	0.0103710
2.00	0.0206085	0.0224262	0.0241890	0.0259020	0.0102341
2.25	0.0201821	0.0219328	0.0236276	0.0252719	0.0101032
2.50	0.0197829	0.0214726	0.0231057	0.0246880	0.0099778
2.75	0.0194078	0.0210417	0.0226186	0.0241444	0.0098575
3.00	0.0190544	0.0206370	0.0221622	0.0236363	0.0097420
3.25	0.0187205	0.0202555	0.0217332	0.0231598	0.0096309
3.50	0.0184042	0.0198951	0.0213288	0.0227115	0.0095240
3.75	0.0181038	0.0195537	0.0209464	0.0222884	0.0094209
4.00	0.0178181	0.0192296	0.0205842	0.0218882	0.0093214
4.25	0.0175457	0.0189212	0.0202401	0.0215088	0.0092253
4.50	0.0172856	0.0186273	0.0199127	0.0211482	0.0091324
4.75	0.0170368	0.0183467	0.0196005	0.0208048	0.0090424
5.00	0.0167984	0.0180783	0.0193024	0.0204773	0.0089553

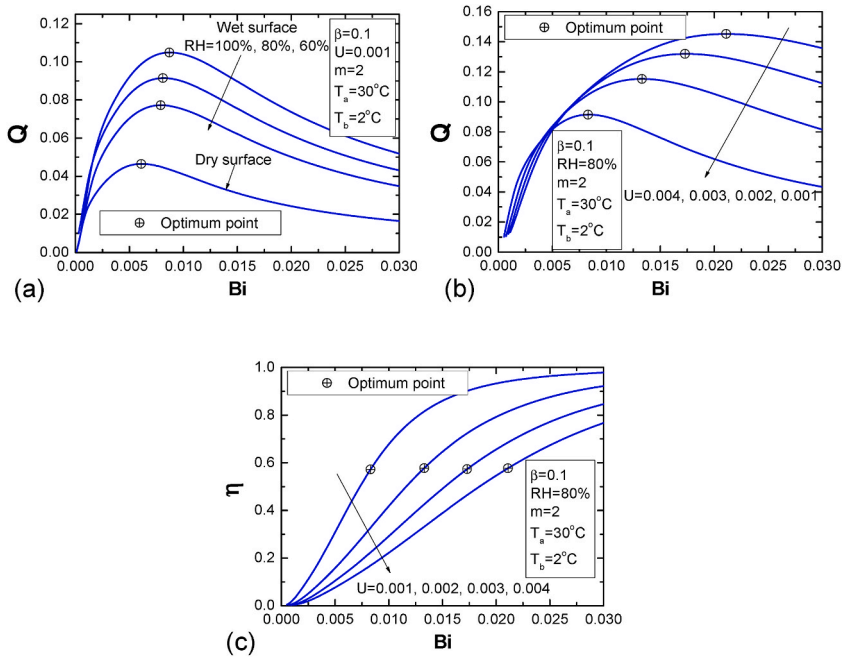

Fig. 9. Heat duty and efficiency of moisten fin dependent on design parameters: (a) Q vs. Bi, (b) Q vs. U, and (c) η vs. Bi.

4. Conclusions

An analytical technique is investigated for the temperature state, efficiency of heat transfer, and optimum dimensions of a moist fin by the actual trend of conduction and convection coefficients along the solid surface. The best fit method is used to evaluate the mass transfer potential in humid air as a nonlinear algebraic equation corresponding to its temperature to include the condensation effect in a realistic approach. The analysis has been carried out for all non-linearity effects associated with such problems. Outcomes from the analysis have been checked with the numerical data to identify the correct status of the model developed. The results predict the surface convection effect is relatively more pronounced compared to the conduction effect on the temperature field, efficiency of

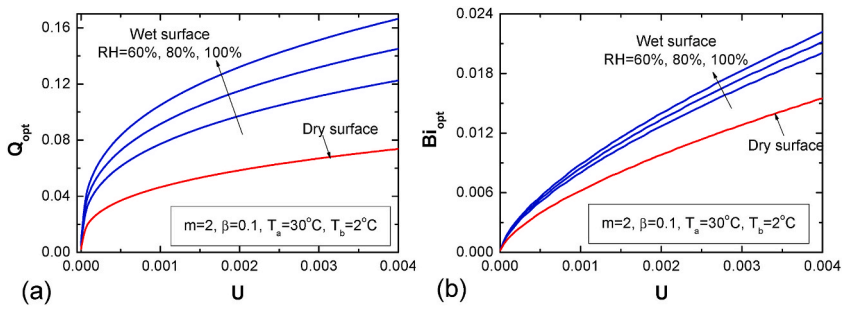

Fig. 10. Extremum design variables for moisten fins with dependability constraint fin volume: (a) Maximum heat transfer duty and (b) Design Biot number.

energy transfer, and extremum design of moistened fins. The fundamental interest of this work is to derive an analytical method for analyzing wet fins with all possible variations of surface heat and mass transfer coefficients as a practical temperature power law. This analysis is well-suitable for the actual design system of moistened fins. The present work draws the following conclusions.

1. A generalized extremum analytical analysis is proposed to predict the design information of moistened fins with all the thermo-physical properties involved in the design with the effect on the temperature scale. Any power-law factor of surface convection coefficients with temperature field is adopted, which can be readily applicable to the actual situation for the energy-exchanging process.
2. The effect of the power index for the variation of convection coefficients on the temperature field, energy transfer performance, and heat load has been investigated extensively. The power index factor for actual variations decreases the fin performance parameters due to the enhancement of thermal resistance for heat flow. The present analytical model has no limitation on the value of the power index to be suitably chosen as per the design requirement.
3. The influence of psychometric properties on the heat transfer parameters for moistened surfaces under nonlinear phenomena for the surface convection effect has been documented.
4. For the actual designed thermal analysis, the optimization is carried out by a general approach satisfying a constraint to be identified based on the design requirement. The optimization study provided the heat load, which is a strong functionality effect on the actual design condition. However, the fin efficiency is almost constant at the optimum point irrespective of practical design circumstances.
5. Finally, the design curves have been drawn to help the investigator for knowing the optimum conditions without the knowledge required for the extensive analysis presented here. The present study is acceptable for dry surface conditions by omitting the latent heat of the condensation term in the proposed mathematical formulations.
6. The present closed-form analysis of moistened fins can be extended easily to analyze the partially wet condition of a fin when required, under a design condition.

Author statement

Balaram Kundu: Conceptualization, Methodology, Software, Validation, Investigation, Formal Analysis, Writing-Original Draft. **Se-Jin Yook:** Conceptualization, Validation, Investigation, Funding acquisition.

Declaration of competing interest

The authors declare that they have no known competing financial interests or personal relationships that could have appeared to influence the work reported in this paper.

Data availability

Data will be made available on request.

References

[1] B. Kundu, Approximate analytic solution for performances of wet fins with a polynomial relationship between humidity ratio and temperature, Int. J. Therm. Sci. 49 (2009) 2108–2118.
[2] Y.T. Lin, K.C. Hsu, Y.J. Chang, Performance of rectangular fin in wet conditions: visualization and wet fin efficiency, J. Heat Tran. 123 (2001) 827–836.
[3] J.L. Threlkeld, Thermal Environmental Engineering, second ed., Prentice-Hall, Englewood Cliffs, New Jersey, 1970.
[4] F.C. McQuiston, Fin efficiency with combined heat and mass transfer, Build. Eng. 81 (1975) 350–355.
[5] A. Kilic, K. Onat, The optimum shape for convecting rectangular fins when condensation occurs, Wärme-und Stoffübertragung 15 (1981) 125–133.
[6] A.H. Elmahdy, R.C. Biggs, Efficiency of extended surfaces with simultaneous heat and mass transfer, Build. Eng. 89 (1983) 135–143.
[7] J.E.R. Coney, C.G.W. Sheppard, E.A.M. El-Shafei, Fin performance with condensation from humid air: a numerical investigation, Int. J. Heat Fluid Flow 10 (1989) 224–231.
[8] J.E.R. Coney, H. Kazeminejad, C.G.W. Sheppard, Dehumidification of air on a vertical rectangular fin: a numerical study, Proc. Inst. Mech. Eng. 203 (1989) 165–175.

[9] V. Srinivasan, R.K. Shah, Fin efficiency of extended surfaces in two-phase flow, Int. J. Heat Fluid Flow 18 (1997) 419–429.
[10] G. Wu, T.Y. Bong, Overall efficiency of a straight fin with combined heat and mass transfer, Build. Eng. 100 (1994) 367–374.
[11] H. Kazeminejad, Analysis of one-dimensional fin assembly heat transfer with dehumidification, Int. J. Heat Mass Tran. 38 (1995) 455–462.
[12] H. Kazeminejad, M.A. Yaghoubi, M. Sepehri, Effect of dehumidification of air on the performance of eccentric circular fins, Proc. Inst. Mech. Eng. 207 (1993) 142–146.
[13] K.T. Hong, R.L. Webb, Calculation of fin efficiency for wet and dry fins, HVAC R Res. 2 (1996) 27–41.
[14] M.M. El-Din Salah, Performance analysis of partially wet fin assembly, Appl. Therm. Eng. 18 (1998) 337–349.
[15] L. Rosario, M.M. Rahman, Overall efficiency of a radial fin assembly under dehumidifying conditions, J. Energy Resour. Technol. 120 (1998) 299–304.
[16] B. Kundu, An analytical study of the effect of dehumidification of air on the performance and optimization of straight tapered fins, Int. Commun. Heat Mass Tran. 29 (2002) 269–278.
[17] G. Sowmya, B.J. Gireesha, H. Berrehal, An unsteady thermal investigation of a wetted longitudinal porous fin of different profiles, J. Therm. Anal. Calorim. 143 (2021) 2463–2474.
[18] P. Naphon, Study on the heat transfer characteristics of the annular fin under dry-surface, partially-wet surface and fully-wet surface conditions, Int. Commun. Heat Mass Tran. 33 (2006) 112–121.
[19] H. Nemati, S. Samivand, Simple correlation to evaluate efficiency of annular elliptic fin circumscribing circular tube, Arabian J. Sci. Eng. 39 (2014) 9181–9186.
[20] M. Turkyilmazoglu, Thermal management of parabolic pin fin subjected to a uniform oncoming airflow: optimum fin dimensions, J. Therm. Anal. Calorim. 143 (2021) 3731–3739.
[21] B. Kundu, Analysis of thermal performance and optimization of concentric circular fins under dehumidifying conditions, Int. J. Heat Mass Tran. 52 (2009) 2646–2659.
[22] M.H. Sharqawy, S. M Zubair, Efficiency and optimization of an annular fin with combined heat and mass transfer - an analytical solution, Int. J. Refrigeration 30 (2007) 751–757.
[23] M.H. Sharqawy, S.M. Zubair, Efficiency and optimization of straight fins with combined heat and mass transfer–an analytical solution, Appl. Therm. Eng. 28 (2008) 2279–2288.
[24] G. Sowmya, B.J. Gireesha, S. Sindhu, Thermal exploration of radial porous fin fully wetted with SWCNTs and MWCNTs along with temperature-dependent internal heat generation, Proc. IMechE Part C: J. Mech. Eng. Sci. 234 (2020) 4945–4952.
[25] A. Moradi, A.P.M. Fallah, T. Hayat, On solution of natural convection and radiation heat transfer problem in a moving porous fin, Arabian J. Sci. Eng. 39 (2014) 1303–1312.
[26] P.K. Roy, A. Mallick, H. Mondal, A modified decomposition solution of triangular moving fin with multiple variable thermal properties, Arabian J. Sci. Eng. 43 (2018) 1485–1497.
[27] C.H. Chiu, C.K. Chen, A decomposition method for solving the convective longitudinal fins with variable thermal conductivity, Int. J. Heat Mass Tran. 45 (2002) 2067–2075.
[28] C. Arslanturk, A decomposition method for fin efficiency of convective straight fins with temperature-dependent thermal conductivity, Int. Commun. Heat Mass Tran. 32 (2005) 831–841.
[29] M.H. Chang, A decomposition solution for fins with temperature dependent surface heat flux, Int. J. Heat Mass Tran. 48 (2005) 1819–1824.
[30] B. Kundu, S.J. Yook, An accurate approach for thermal analysis of porous longitudinal, spine and radial fins with all nonlinearity effects–analytical and unified assessment, Appl. Math. Comput. 402 (2021), 126124.
[31] A. Vahabzadeh, D.D. Ganji, M. Abbasi, Analytical investigation of porous pin fins with variable section in fully-wet conditions, Case Stud. Therm. Eng. 5 (2015) 1–12.
[32] H.S. Peng, C.L. Chen, Hybrid differential transformation and finite difference method to annular fin with temperature dependent thermal conductivity, Int. J. Heat Mass Tran. 54 (2011) 2427–2433.
[33] G. Domairry, M. Fazeli, Homotopy analysis method to determine the fin efficiency of convective straight fins with temperature dependent thermal conductivity, Commun. Nonlinear Sci. Numer. Simulat. 14 (2009) 489–499.
[34] M. Babaelahi, M.R. Raveshi, Analytical efficiency analysis of aerospace radiating fin, Proc. IMechE Part C: J. Mech. Eng. Sci. 228 (2014) 3133–3140.
[35] I. Rusagara, C. Harley, Mean action time as a measure for fin performance in one dimensional fins of exponential profiles, Appl. Math. Comput. 238 (2014) 319–328.
[36] E. Cuce, M.P. Cuce, Homotopy perturbation method for temperature distribution, fin efficiency and fin effectiveness of convective straight fins with temperature-dependent thermal conductivity, Proc. IMechE Part C: J. Mech. Eng. Sci. 227 (2012) 1754–1760.
[37] S.W. Ma, A.I. Behbahani, Y.G. Tsuei, Two-dimensional rectangular fin with variable heat transfer coefficient, Int. J. Heat Mass Tran. 34 (1991) 79–85.
[38] I.N. Dul'kin, G.I. Garas'ko, Analysis of the 1D heat conduction problem for a single fin with temperature dependent heat transfer coefficient: part I extended inverse and direct solutions, Int. J. Heat Mass Tran. 51 (2008) 3309–3324.
[39] I.N. Dul'kin, G.I. Garas'ko, Analysis of the 1D heat conduction problem for a single fin with temperature dependent heat transfer coefficient: part II optimum characteristics of straight plate and cylindrical pin fins, Int. J. Heat Mass Tran. 51 (2008) 3325–3341.
[40] L.T. Yu, C.K. Chen, Optimization of circular fins with variable thermal parameters, J. Franklin Inst. 336 (1999) 77–95.
[41] C.Y. Lai, H.S. Kou, J.J. Lee, Recursive formulation on thermal analysis of an annular fin with variable thermal properties, Appl. Therm. Eng. 29 (2009) 779–786.
[42] F. Khani, A. Aziz, Thermal analysis of a longitudinal trapezoidal fin with temperature-dependent thermal conductivity and heat transfer coefficient, Commun. Nonlinear Sci. Numer. Simulat. 15 (2010) 590–601.
[43] B. Kundu, S. Wongwises, A decomposition analysis on convecting-radiating rectangular plate fins for variable thermal conductivity and heat transfer coefficient, J. Franklin Inst. 349 (2012) 966–984.
[44] A.Y. Adam, A.N. Oumer, G. Najafi, M. Ishak, M. Firdaus, T.B. Aklilu, State of the art on flow and heat transfer performance of compact fin-and-tube heat exchangers, J. Therm. Anal. Calorim. 139 (2020) 2739–2768.
[45] S.E. Ghasemi, M. Hatami, D.D. Ganji, Thermal analysis of convective fin with temperature-dependent thermal conductivity and heat generation, Case Stud. Therm. Eng. 4 (2014) 1–8.
[46] M. Turkyilmazoglu, Exact solutions to heat transfer in straight fins of varying exponential shape having temperature dependent properties, Int. J. Therm. Sci. 55 (2012) 69–75.
[47] M. Turkyilmazoglu, Efficiency of heat and mass transfer in fully wet porous fins: exponential fins versus straight fin, Int. J. Refrigeration 46 (2014) 156–164.
[48] G.L. Standart, S.N. Husaini, Condensation of a pure vapor on a longitudinal fin mounted on a vertical tube, Chem. Eng. J. 10 (1975) 173–187.
[49] T.H. Chilton, A.P. Colburn, Mass transfer (absorption) coefficients: prediction from data on heat transfer and fluid friction, Ind. Eng. Chem. 26 (1934) 1183–1187.
[50] S.Y. Liang, T.N. Wong, G.K. Nathan, Comparison of one-dimensional and two-dimensional models for wet surface fin efficiency of a plate-fin-tube heat exchanger, Appl. Therm. Eng. 20 (2000) 941–962.
[51] G. Adomian, Non-linear Stochastic Systems: Theory and Applications to Physics, Kluwer Academic Publishers, Netherlands, 1989.
[52] S.D. Hwang, H.G. Kwon, H.H. Cho, Local heat transfer and thermal performance on periodically dimple-protrusion patterned walls for compact heat exchangers, Energy 35 (2010) 5357–5364.
[53] H. Sadeghifar, A.K.S. Kordi, A new and applicable method to calculate mass and heat transfer coefficients and efficiency of industrial distillation columns containing structured packings, Energy 36 (2011) 1415–1423.
[54] B. Kundu, K.S. Lee, Analytic solution for heat transfer of wet fins on account of all nonlinearity effects, Energy 41 (2012) 354–367.